

Neuronal Correlates of Local, Lateral, and Translaminar Inhibition with Reference to Cortical Columns

Moritz Helmstaedter¹, Bert Sakmann¹ and Dirk Feldmeyer^{1,2,3}

¹Department of Cell Physiology, Max-Planck Institute for Medical Research, Jahnstrasse 29, D-69120 Heidelberg, Germany, ²Current address: Research Centre Jülich, Institute for Neuroscience and Biophysics, INB-3 Medicine, Leo-Brandt-Strasse, D-52425 Jülich, Germany and ³Current address: Department of Psychiatry and Psychotherapy, RWTH Aachen University, Pauwelsstrasse 30, D-52074 Aachen

In the neocortex, inhibition by γ -aminobutyric acidergic (GABAergic) interneurons is essential for shaping cortical maps, which represent sensory signals. For a detailed understanding of the stream of excitation evoked, for example, by a sensory stimulus, interneurons must be identified with reference to their impact on excitatory neurons located in different laminae of the same (home) and surround columns. We analyzed the axonal projection of layer 2/3 (L2/3) interneurons with reference to geometric landmarks of cortical columns by staining neurons in acute slices of rat barrel cortex (P20–P29) and a subsequent cluster analysis using morphological parameters that described the spatial distribution of axons. The cluster analysis defined 4 main axonal projection “types” referred to as 1) “local inhibitors” (including “chandelier neurons”), 2) “lateral inhibitors,” 3) “translaminar L2/3-to-L4/5 inhibitors,” and 4) “translaminar L2/3-to-L1 inhibitors.” The putative innervation domains established by axonal projections of the 4 types of interneurons and the dendritic domains of their target excitatory neurons were 1) L2/3 of the home column, 2) L2/3 of both the home and neighboring columns, 3) L4 and L5A of the home column, and 4) L1 and L2/3 of the home column. The quantitative analysis of the axonal projection patterns of an unselected sample of 51 interneurons located in L2/3 thus defined anatomical correlates for local, lateral, and translaminar inhibition within and between cortical columns.

Keywords: axon, barrel cortex, cluster analysis, cortical column, GABAergic interneuron, lateral inhibition, layer 2/3

Introduction

The concept of cortical columns as basic functional units in the neocortex postulates neuronal ensembles of approximately 10^4 cells to comprise representational modules in primary sensory areas (Mountcastle 1957, 1997, 2003; Woolsey and Van der Loos 1970; Lübkke et al. 2003; Helmstaedter et al. 2007; for a critical review, see Douglas and Martin 2007). The majority of these cells evoke excitatory postsynaptic potentials in their target neurons. Anatomically they have pyramidal or spiny stellate soma-dendritic shapes (Lund 1973; Van Essen and Kelly 1973; Gilbert and Wiesel 1979). Approximately 10–20% are nonpyramidal γ -aminobutyric acidergic (GABAergic) neurons that evoke chloride-mediated, inhibitory postsynaptic potentials (IPSPs; Jones 1975; Houser et al. 1983; Beaulieu et al. 1992; for a review, see Soltesz 2006). Sensory-evoked responses in supragranular layers are dominated by glutamate-mediated depolarization (Brecht et al. 2003). However, inhibition affects the time course of the subthreshold compound Postsynaptic Potential (PSP), the timing of action potentials (APs) (Larkum et al. 1999; Pouille and Scanziani 2001), and is required for shaping the complex receptive field properties in visual and

somatosensory cortices (Rose and Blakemore, 1974; Sillito 1975; Kyriazi et al. 1996; Hensch et al. 1998; Hausser et al. 2000; Pinto et al. 2000, 2003).

AP rates in response to sensory stimuli are low in layer 2/3 (L2/3) of barrel cortex (Brecht et al. 2003; deKock et al. 2007; Kerr et al. 2007). Suppression of principal whisker responses after surround whisker deflection has been suggested based on voltage-sensitive dye imaging in supragranular layers (Kleinfeld and Delaney 1996; Goldreich et al. 1998). Voltage-sensitive dye imaging also allowed the direct observation of putative surround inhibition in response to principal whisker deflection (Derdikman et al. 2003). “Local inhibition” within a column together with “lateral inhibition” across columns could account for these observations.

Here we aimed at identifying putative neuronal correlates of local and lateral inhibition within and between cortical columns. We therefore analyzed axonal projections of interneurons with the clearly discernible cortical columns in the somatosensory (barrel) cortex of rodents as the reference structure for geometric analysis.

Axonal projections have been previously described qualitatively (for an overview, see Fairén et al. 1984). Quantitative descriptions of axonal projections have focused on local branching geometry (Karube et al. 2004) and on the extent of the axonal field in the absence of anatomical landmarks (Valverde 1976; Blatow et al. 2003; Karube et al. 2004; Krimer et al. 2005; Dumitriu et al. 2007). For pyramidal neurons with long-range axonal projections to other cortical areas or subcortical structures, axonal projections can be analyzed with a coarse spatial reference (such as cortical areas or subcortical structures). For locally projecting interneurons, however, with axonal projections refined to parts of a cortical area (such as single columns, e.g., in the barrel field), the choice of the spatial reference used for the analysis of axonal projections is more critical. The axonal field of interneurons has been used previously to infer projection types, with sole reference to the soma of the interneuron in the absence of anatomical landmarks (e.g., Valverde 1976).

We investigated whether axonal projections of interneurons were in fact specific with reference to functional landmarks, the columns in rat barrel cortex. We show that the position of the soma within a column is relevant for the type of axonal projection. We conclude that the relevant reference for the analysis of axonal projections of interneurons is functional landmarks, such as cortical columns.

We then defined specific axonal projection patterns in relation to the borders and laminae of cortical (barrel) columns. The quantitative measures of axonal projection patterns were derived based on 51 computer-aided reconstructions of

dendritic and axonal arbors of interneurons located in L2/3. An unsupervised cluster analysis defined 4 main types of interneurons by their axonal projection: in addition to local and lateral inhibitors, we found L1 inhibitors and translaminal L2/3-to-L4/5 inhibitors. The 4 axonal projection types of interneurons were mapped onto the dendritic domain of putative postsynaptic target cells to reveal specific inhibitory innervation domains within and across cortical columns.

In subsequent studies, we investigated the relation of dendritic geometry and intrinsic electrical excitability to the “axonal projection types” described in this study (Helmstaedter et al. 2008a, 2008b). We also analyzed the synaptic input from L4 to these types of interneurons (Helmstaedter, Staiger, et al. 2008).

Materials and Methods

Preparation

All experimental procedures were performed according to the animal welfare guidelines of the Max-Planck Society. Wistar rats (20–29 days old) were anesthetized with isoflurane and decapitated, and slices of somatosensory cortex were cut in cold extracellular solution using a vibrating microslicer (DTK-1000; Dosaka, Kyoto, Japan). Slices were cut at 350- μ m thickness in a thalamocortical plane (Agmon and Connors 1991) at an angle of 50° to the interhemispheric sulcus. Slices were incubated at room temperature (22–24 °C) in an extracellular solution containing 4 mM MgCl₂ and 1 mM CaCl₂ to reduce synaptic activity.

Solutions

Slices were continuously superfused with an extracellular solution containing (in millimolar (mM)) the following: 125 NaCl, 2.5 KCl, 25 glucose, 25 NaHCO₃, 1.25 NaH₂PO₄, 2 CaCl₂, and 1 MgCl₂ (bubbled with 95% O₂ and 5% CO₂). The pipette (intracellular) solution contained (in mM) the following: 105 K-gluconate, 30 KCl, 10 4-(2-hydroxyethyl)-1-piperazineethanesulfonic acid, 10 phosphocreatine, 4 ATP-Mg, and 0.3 GTP (adjusted to pH 7.3 with KOH); the osmolarity of the solution was 300 mOsm. Biocytin (Sigma, Munich, Germany) at a concentration of 3–6 mg/mL was added to the pipette solution, and cells were filled during 1–2 h of recording.

Identification of Barrels and Neurons

Slices were placed in the recording chamber and inspected with a 2.5 \times /0.075 NA Plan objective using bright-field illumination. Barrels were identified as narrow dark stripes with evenly spaced, light “hollows” (Agmon and Connors 1991; Feldmeyer et al. 1999) and photographed using a frame grabber for later analysis. Interneurons were searched in L2/3 above barrels of 250 \pm 70 μ m width ($n = 64$) using a water 40 \times /0.80 NA objective and infrared-differential interference contrast microscopy (Dodt and Zieglgänsberger 1990; Stuart et al. 1993). Somata of neurons in L2/3 were selected for recording if a single apical dendrite was not visible. This was the only criterion for the a priori selection of interneurons. Whole-cell recordings and simultaneous biocytin fillings were made using patch pipettes of \sim 5 to 8 M Ω resistance pulled of thick borosilicate glass capillaries (outer diameter: 2.0 mm, inner diameter: 0.5 mm; F. Hilgenberg, Malsfeld, Germany). After recording, the pipettes were positioned above the slice at the position of the recorded cells, and the barrel pattern with the pipettes visible was again photographed using bright-field illumination.

Histological Procedures

After recording, slices were fixed at 4 °C for at least 24 h in 100 mM phosphate buffer, pH 7.4, containing either 4% paraformaldehyde or 1% paraformaldehyde and 2.5% glutaraldehyde. Slices containing biocytin-filled neurons were processed using a modified protocol described previously (Lübke et al. 2000). Slices were incubated in 0.1% Triton X-100 solution containing avidin-biotinylated horseradish peroxidase (ABC-Elite; Camon, Wiesbaden, Germany); subsequently, they were

reacted using 3,3-diaminobenzidine as a chromogen under visual control until the dendritic and axonal arborization was clearly visible. To enhance staining contrast, slices were occasionally postfixed in 0.5% OsO₄ (30–45 min). Slices were then mounted on slides, embedded in Mowiol (Clariant, Sulzbach, Germany), and enclosed with a coverslip.

Reconstruction of Neuronal Morphologies

Subsequently, neurons were reconstructed with the aid of NeuroLucida software (MicroBrightField, Colchester, VT) using an Olympus Optical (Hamburg, Germany) BX50 microscope at a final magnification of 1000 \times . Only neurons with sufficient dendritic and axonal staining (total axonal path length $>$ 4 mm) were used for analysis. The reconstructions provided the basis for the quantitative morphological analysis (see below). The pial surface of the slice was also traced. The reconstruction was rotated in the plane of the slice such that the pial surface above the reconstructed neuron was horizontally aligned.

Quantitative Analysis of Axonal Projections

First, barrel outlines and layer borders were visually identified in the bright-field photographs taken before the recordings. Then the photographs taken after the recording were aligned visually, and the tips of the pipettes were taken as the locations of the somata relative to the barrel pattern. Column borders were extrapolated from the lateral borders of the barrels approximated as straight lines. Layer borders were defined by curved lines approximating the curvature of the cortex in the field of view. Care was taken to rotate the barrel image such that the pial surface above the recording location was aligned horizontally. This resulted in a grid defining layer borders horizontally and column borders vertically. This grid was used by custom-made software (RembrandtII) written in Igor Pro (Wavemetrics, Lake Oswego, OR) to extract the relative coordinates of the soma positions and the layers and borders of the cortical columns in the thalamocortical slice plane.

Second, the reconstruction of the neuronal morphology as generated by the NeuroLucida software (represented as lists of 3D cylinder segments) was read-in by the custom-made software RembrandtII. The 3D path lengths of all cylinder segments of one neuron's axon were sampled into a 2D map of 10 \times 10- μ m square voxels in the plane of the slice, representing a 2D map of axonal length density (map 1). Map 1 was then aligned to the grid representing the soma location and the borders of layers and columns. In most cases, 2 neurons were recorded in one slice (paired recordings of L2/3 interneurons and L4 spiny neurons were made to determine the synaptic input of L2/3 interneurons [Helmstaedter, Staiger et al. 2008]). In these cases, the locations of the 2 somata (separated by 150–650 μ m) were used for the alignment of the column layer grid with the reconstruction. If only one neuron was recorded in one slice, the soma location and the pial surface were used for alignment.

Then axonal path lengths were measured by integration of map 1 in regions defined by the borders and layers of the cortical columns, yielding a maximum resolution of 10 μ m.

Then map 1 was sampled into a corresponding 2D map at 50- μ m resolution (map 2) corresponding to a spatial low-pass filtering. Map 2 was convolved with a Gaussian function (standard deviation 50 μ m) and then interpolated 10-fold in both dimensions. The resulting interpolated map of axonal length density (map 3) was used to compute contour lines that represent an average outline of the axonal projection of a single neuron. The “90% contour lines” were computed as isodensity lines that enclosed 90% of the total axonal length of the neuron.

Laterality

The “laterality” of the axonal projection was defined by 2 measures: 1) the ratio of the total axonal path length of a neuron that extended outside of the home column, η_{lat} (cf., Fig. 1B). The home column was here defined to include the adjacent septa in order to reduce variability in determining the lateral borders of the home column due to the thalamocortical slice plane. Thus, the “lateral” part of the axon as defined here was certainly not located in the home column. The average width of the home columns as defined here was 366 \pm 80 μ m

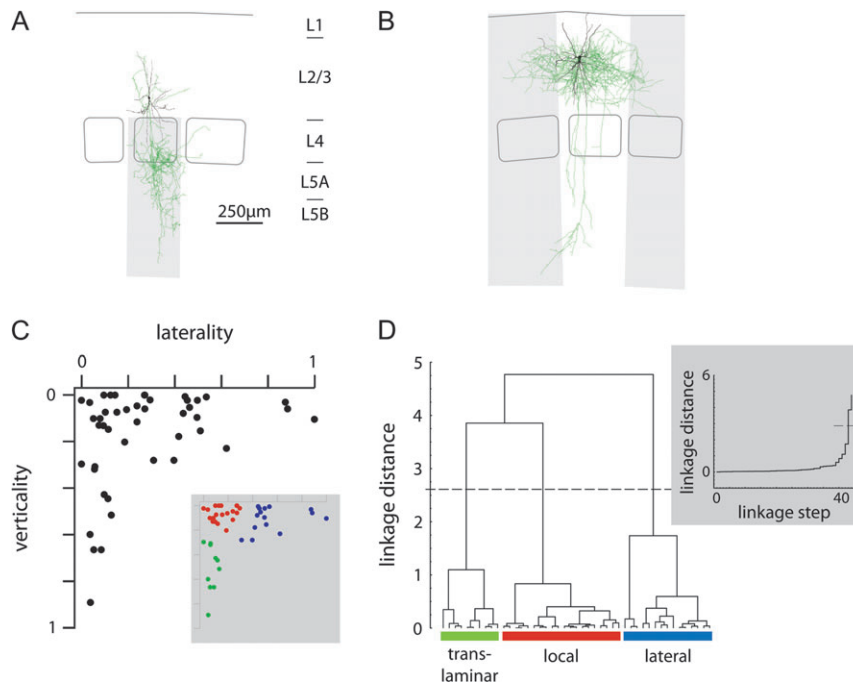


Figure 1. Quantitative analysis of axonal projection domains. (A) Reconstruction of a L2/3 interneuron from rat barrel cortex. Soma and dendrites, black; axon, green. The verticality of axonal projection was defined as the ratio of axonal path length that extended below the upper border of L4 (gray area). (B) Reconstruction of a L2/3 interneuron, same color code as in (A). The laterality of axonal projection was defined as a linear combination of the ratio of axonal path length extending beyond the home column and the adjacent septa (gray area), and the total lateral extent of the axonal projection measured in units of home column width (for details cf., Materials and methods). (C) Distribution of laterality and verticality of axonal projections of 45 L2/3 interneurons. The inset shows clusters that were determined by a cluster analysis (Euclidean distances, Ward's linkage method; Ward 1963). (D) The linkage dendrogram for the cluster analysis. The dashed line indicates the cutoff as determined by Thorndike's procedure (Thorndike 1953); the inset shows the plot of linkage distance versus linkage step. The maximum increase in linkage distance is determined as linkage cutoff. The resulting 3 clusters are coded in red, blue, green, and respectively, and are designated local, lateral, and translaminar L2/3-to-L4/5 inhibitors, respectively.

($n = 51$). The average septum width was $56 \pm 26 \mu\text{m}$. 2) The total horizontal extent of the axon $dx_{90\text{lat}}$. This measure was calculated as the horizontal extent of the 90% contour of the axon (see above) in units of the width of the home column. Here, the width of the home column was defined to include half of the adjacent septa for symmetry reasons. Use of the low-pass filtered 90% contour rather than the detailed axonal morphology reduced the sensitivity of this measure to single branches of the axon. The 2 measures of laterality were combined to a single measure of axonal laterality $\alpha_{x\text{lat}}$ by normalizing to the maximal value and projection on a principal axis:

$$\alpha_{x\text{lat}} = \frac{w_{\text{lat}} \times r_{\text{lat}} / \max(r_{\text{lat}}) + w_{dx_{90\text{lat}}} \times dx_{90\text{lat}} / \max(dx_{90\text{lat}})}{(w_{\text{lat}} + w_{dx_{90\text{lat}}})}$$

with the parameter weights w_{lat} and $w_{dx_{90\text{lat}}}$ set to 1 and 2, respectively, to approximate the first principal axis of the 2 parameters.

Verticality

The verticality of the axonal projection was defined as the ratio of the axon that was located below the L4-to-L2/3 border in the home column.

Cluster Analysis

Axonal projection types were determined using a cluster analysis in the 2D parameter space of axonal laterality and axonal verticality as defined above. Distances were measured as Euclidean, and a linkage method based on the minimal increase of intracluster variance at each linkage step was used (Ward's method; Ward 1963). For determining the number of clusters present, the Thorndike procedure was used (Thorndike 1953; Cauli et al. 2000). Briefly, the linkage step leading to the maximum increase in linkage distance was used for cutoff. The clustering was not altered if both measures of laterality were used for distance measurement together without projection on a principal axis (clustering in 3D space).

Definition of L1 Inhibitors

For the definition of L1 inhibitors, 2 parameters were quantified for each neuron: 1) the fraction of the total axonal path length of a single interneuron extending in layer 1 (L1) and 2) the total path length of the axon in L1. A cluster analysis (Euclidean distances, Ward's linkage method, Thorndike procedure for definition of number of clusters) was made in the 2D space of these 2 parameters.

Definition of Chandelier Neurons

Chandelier neurons (Szentagothai and Arbib 1974; Jones 1975; Somogyi 1977; Somogyi et al. 1982; for a review, see Howard et al. 2005) were identified qualitatively by visual inspection, only. The axon of the chandelier neurons formed >100 branches of approximately 10–20- μm length each that were oriented perpendicular to the pial surface. This axonal feature was clearly separable in the sample of interneurons.

Average Maps of Axonal Length Density

The interpolated maps of axonal length density ("map 3," cf., above) generated for each neuron were averaged for all neurons of the same axonal projection type. The single-neuron maps were translated before summing, such that the center of the home barrel of each map was aligned to the center of the average home barrel. The 90% contour line was calculated for the averaged density map.

Average Barrel Outlines

The average axonal density maps were superimposed with the average barrel outlines that were determined as follows: The grids of layers and column borders for all neurons of a common axonal projection type were aligned to the centers of the respective home barrels. Then, the outlines of barrels were approximated by 4 corner points connected by straight lines, respectively. The corner point coordinates were then

averaged for the different types of cells. The average axonal path lengths measured in the different layers of the home and neighboring columns are reported in the Supplementary material (Supplementary Table 1).

Average Maps of Innervation Probabilities

“Innervation domains” were calculated for 2 putative types of target neurons: L2/3 pyramidal cells and L4 spiny neurons. Reconstructions of the dendritic trees of 25 L2/3 pyramidal cells (Lübke et al. 2003; Feldmeyer et al. 2006; Helmstaedter et al. 2008a) and 36 L4 spiny neurons were processed as described above to obtain average interpolated maps of dendritic length density aligned to the center of the home barrel. For each of the axonal projection types, the barrel-aligned average axonal density maps were pointwise multiplied to the barrel-aligned average dendritic density maps. All maps were not normalized, so the product density was comparable among types. Three contour lines at the same absolute product density are shown for all innervation domains for comparison (Fig. 6). For chandelier neurons, instead of average maps of dendritic trees, average maps of axonal initial segment length were calculated. For each of the 25 L2/3 pyramidal neurons and the 36 L4 spiny neurons, 20- μm length of the putative axonal initial segment length was assumed at the location of the soma in the 50- μm map, aligned to the center of the barrel. The map was then convolved and interpolated as described above.

Results

A post hoc analysis of a sample of 64 whole-cell recordings of L2/3 nonpyramidal cells in P20–P29 rat barrel cortex was made to identify the distribution of projection patterns of inhibitory cells with as little preselection bias as possible. Paired recordings from L4 and L2/3 neurons were made to define the excitatory input to these interneurons (Helmstaedter, Staiger, et al. 2008). For a subset of 51 recordings, the staining of axonal arbors was sufficiently complete to allow a detailed computer-aided reconstruction and the measurement of axonal projections with reference to the columnar pattern as delineated by barrels in layer 4 (cf., Materials and methods). Two of the 51 neurons were classified as chandelier neurons, and 4 of 51 neurons were defined as L1 inhibitors based on quantitative criteria as detailed below. The majority (45 of 51 neurons) could not be defined by these simple criteria and were therefore subject to an unsupervised cluster analysis evaluating the lateral and vertical axonal projections of the interneurons. This analysis is described first.

Laterality and Verticality of Axonal Projections

The distribution of axonal path lengths of L2/3 interneurons was analyzed in regions outlined by the presumed pattern of columns in the vertical (along the column axis) and lateral (horizontal) directions (cf., Materials and methods). Figure 1A,B shows 2 examples where the “verticality” of axonal projection within the home column was defined as the ratio of axonal length entering layer 4 and lower layers (Fig. 1A, gray box). As a measure of “laterality,” the ratio and the horizontal extent of the axonal projection outside the home column were quantified and projected onto an idealized scale (gray box in Fig. 1B, for details, see Materials and methods). The distribution of laterality and verticality for the 45 interneuron axons is shown in Figure 1C. A cluster analysis (Cauli et al. 2000) revealed 3 clusters of axonal projections with reference to cortical columns (Fig. 1D; Ward’s method, the Thorndike procedure suggests 3 clusters, cf., inset and Materials and methods). These 3 clusters were designated as 3 types of axonal projections: *local inhibitors* (Fig. 1C, red circles),

lateral inhibitors (Fig. 1C, blue circles), and vertically projecting *translaminar L2/3-to-L4/5 inhibitors* (Fig. 1C, green circles). Figure 2 shows the overlay of the reconstructions for the corresponding types. These types are discussed along with their corresponding average length density maps below.

Relation between Soma Location, Axonal Field Span, and Laterality

We then investigated whether the axonal projection to neighboring columns was caused primarily by a broad axonal field span in the horizontal direction or by the position of the soma at the borders of a column. Figure 3A shows the relation between the ratio of the axon that was extended to the neighboring columns and the horizontal field span of the axon. For a broad range of axonal field spans (range 300–600 μm), the ratio of the axon that was extended to the neighboring columns varied between highly local (<10% laterality ratio) and significantly lateral (>30% laterality ratio) projections. Figure 3B shows the relation between the ratio of the axon that was extended to the neighboring columns and the horizontal position of the soma within the home column (gray shading indicates range of the home column). Interneurons with significant projection to neighboring columns (laterality ratio >30%) had a clear tendency to be located at the border of the home column (within the outer 20% of the column radius). We conclude that 1) the position of the interneuron soma within a column mattered for the type of axonal projection and 2) that the axonal field span alone could not be used to predict axonal projections with reference to cortical columns.

Axonal Projection to L1

We further quantified the ratio of axonal length extending into L1. Extensive axonal projections to L1 have been previously suggested to be a specific property of a class of interneurons (Martinotti 1889; Ramón y Cajal 1904; Fairén et al. 1984; Karube et al. 2004; Wang et al. 2004). Figure 4A shows the reconstruction of a L2/3 interneuron with significant projections to L1 (gray box). We measured 2 parameters to quantify the projections to L1: 1) the fraction of axonal length in L1 and 2) the total axonal length in L1. (Fig. 4B). A cluster analysis yielded the definition of an additional type of L2/3 interneurons: L1 inhibitors as nonpyramidal cells with >30% of their total axonal projection extending to L1 (Fig. 4C). The average projection pattern of the 4 L1 inhibitors we found in the sample is shown in Figure 4D as overlay.

Chandelier Neurons

The sample contained 2 interneurons that had the striking feature of several hundreds of vertically oriented axonal segments (Fig. 5B). These cells were described as chandelier cells and have been shown to target axon initial segments of pyramidal neurons in visual and motor cortices of rat, cat, and monkey (Szentagothai and Arbib 1974; Somogyi 1977; Somogyi et al. 1982; Gonchar et al. 2002; for a review, see Howard et al. 2005). The reconstructions revealed that both cells were confined to the home column (Fig. 5A) with a vertical delineation of the lateral extent of the axonal projection at the border of the home column. The chandelier neurons were

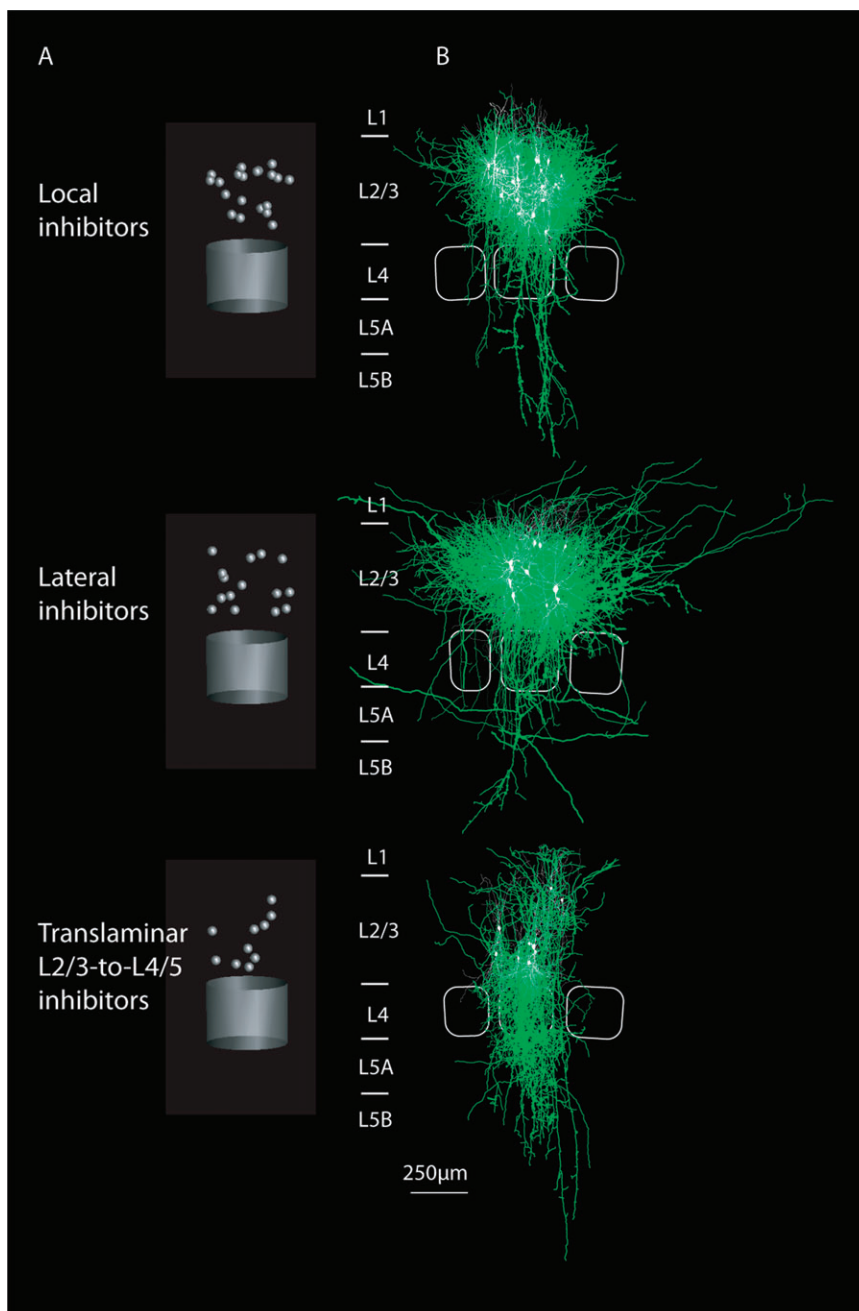


Figure 2. Soma locations and average axonal projections of local, lateral, and translaminal L2/3-to-L4/5 inhibitors with reference to cortical columns. (A) Schematic indication of the recorded soma locations depicted in a normalized cortical column (distance of upper L4 border to L1 border approximately equals the width of column plus adjacent septa, 400 ± 40 vs. 370 ± 85 μm). Soma locations perpendicular to the slice plane were drawn from a random distribution within the measured column radius. (B) Overlay of dendritic and somatic reconstructions sorted by the type of axonal projection as determined by cluster analysis (Fig. 1). Axons, green; dendrites and somata, white. Top, local; middle, lateral; bottom, translaminal L2/3-to-L4/5 inhibitors. The average barrel outlines are drawn in light gray.

thus interpreted as a group of local inhibitors with specific properties of their axonal arbor.

Axonal Length Density Maps

The single-cell geometries of local, lateral, and translaminal L2/3-to-L4/5 inhibitors were superimposed (Fig. 2), and average axonal length density maps were constructed with reference to the outline of an average cortical column (Fig. 6A).

Local inhibitors showed an axonal projection largely confined to L2/3 of the home column (including the septum),

as is apparent in the average density plot (Fig. 6A, upper panel). Their locality exceeded 80%, quantified as the fraction of axonal length projecting to L2/3 of the home column, with an average total axonal length of 18 ± 9 mm ($n = 20$, cf., Table 1).

Lateral inhibitors showed clear transcolumar projections within L2/3, as indicated by the contour line enclosing 90% of the total axonal projection spanning on average 3 columns (Fig. 6A, middle panel). The a-posteriori analysis of this type of interneurons revealed cells with either >2 columns lateral extent or $>30\%$ axon outside the home column. The total

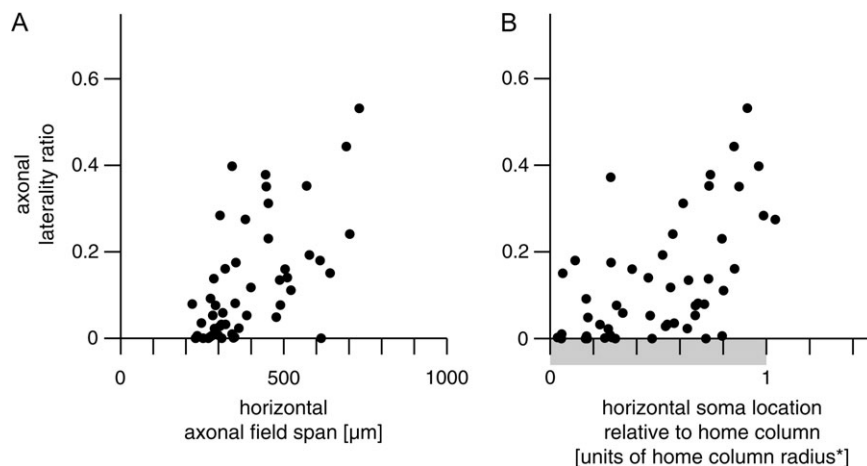


Figure 3. Relation between axonal field span, laterality of axonal projection, and soma location in a column. (A) Relation between the ratio of axonal path length extended to neighboring columns (“axonal laterality ratio,” cf., Materials and methods) and the horizontal axonal field span measured as the horizontal extent of the isodensity contour containing 80% of a single neuron’s axonal projection (cf., Materials and methods; $r_s = 0.63$, $P < 10^{-4}$). For a broad range of axonal field spans (ca., 300–600 μm), the axonal laterality ratio varied between $<10\%$ (a highly local axonal projection) and $>30\%$ (a significantly lateral axonal projection). Thus, axonal field span could not serve as a surrogate parameter for the laterality of axonal projection (cf., Results and Discussion). (B) Relation between the ratio of axonal path length extending to neighboring columns (as in A) and the position of the soma along the horizontal axis within the home column ($r_s = 0.56$, $P < 10^{-4}$). The horizontal soma position was measured relative to the radius of the home column (for details, cf., Materials and methods) and was rendered symmetrical such that “0” corresponds to the center of the home column and “1” corresponds to the border of the home column (for details, cf., Materials and methods). Interneurons with significant axonal projection to neighboring columns (axonal laterality ratio $>30\%$) had a tendency to be located close to the border of the home column (relative horizontal position >0.7). Note, however, that a large fraction of neurons located at the home column border also had purely local axonal projections (axonal laterality ratio $<10\%$).

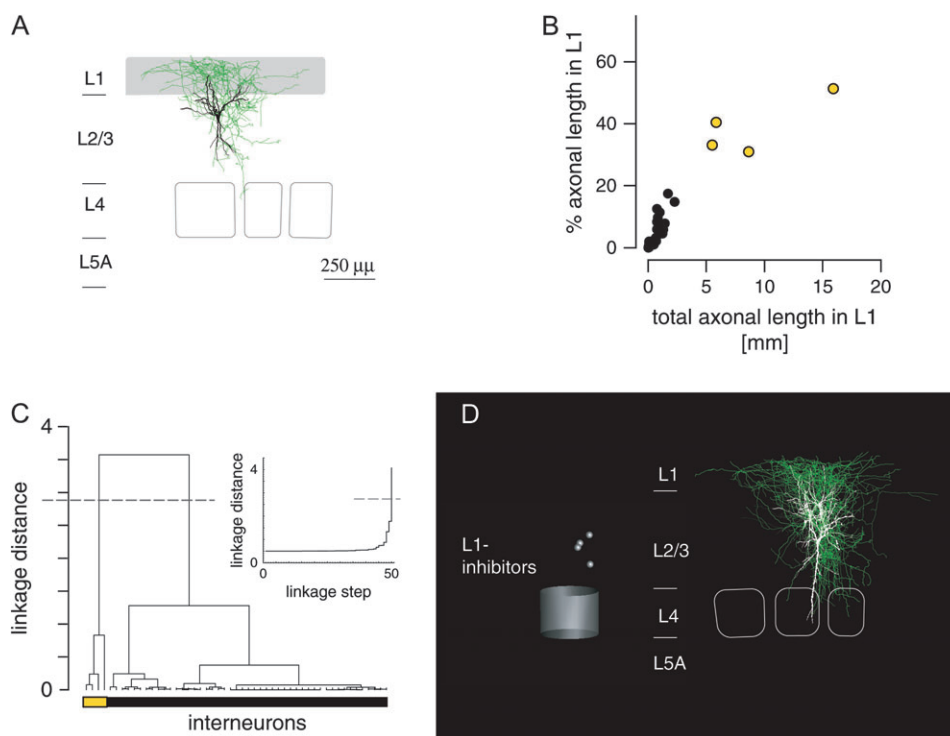


Figure 4. Quantitative analysis of axonal projections to L1. (A) Reconstruction of an interneuron with extensive projections to L1. The L1 projection ratio was determined as the ratio of axonal path length extended into L1 (gray area). Color code as in Figure 1. (B) Distribution of L1 projection ratio and total axonal path length extended to L1 for the sample of 51 interneurons. Note that most (47 of 51) neurons showed virtually no axonal projection to L1 (black circles, only $3 \pm 4\%$ L1 projection ratio and 420 ± 550 - μm axonal path length in L1). (C) A cluster analysis defines a small cluster of 4 neurons with more than 30% and more than 5 mm of axon extended to L1 (Ward’s method, Euclidean distances, Thorndike procedure for cluster cutoff). (D) Soma positions (left panel) and overlay of reconstructions of the 4 L1 inhibitors found in the sample.

axonal length of lateral inhibitors was 24 ± 12 mm ($n = 15$, cf., Table 1).

Translaminar L2/3-to-L4/5 inhibitors showed dense projections to layer 4 and infragranular layers 5A,B of the home

column (Fig. 2B, lower panel). The average density plot revealed that the peak of the axonal projection is within layer 4 (Fig. 6A, lower panel), in strong contrast to local and lateral inhibitors. In addition, the axonal projection of translaminar

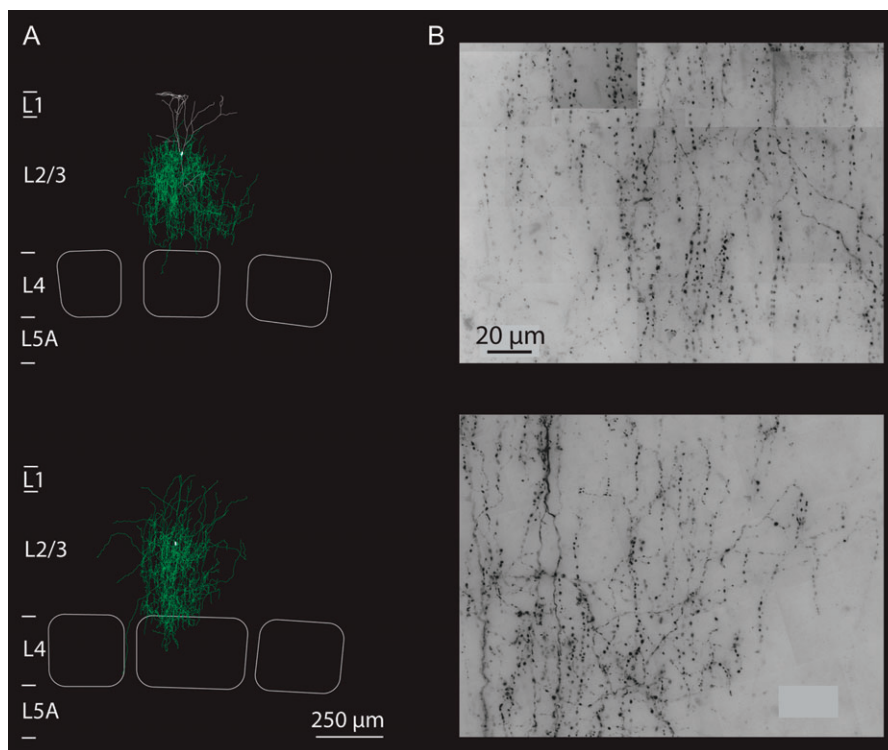


Figure 5. Chandelier neurons. (A) Reconstructions and barrel patterns for 2 chandelier neurons found in the sample. Note the confinement of axonal projection to the home column (axon colored green). (B) Representative images of the diamino-benzidine-stained axons of the 2 neurons (z projections of bright-field images). The sections show approximately 40–50 vertically oriented axonal segments from part of the axonal tree. Scale bar applies to both panels.

L2/3-to-L4/5 inhibitors showed columnar confinement, which could be asymmetric toward the home column as for the cell depicted in Figure 1A. The total axonal length of translaminal L2/3-to-L4/5 inhibitors was 14 ± 11 mm ($n = 10$, cf., Table 1).

Innervation Patterns

To quantify putative postsynaptic targeting patterns of L2/3 interneurons, we used dendritic density maps of L2/3 pyramidal cells and L4 spiny neurons in order to construct probability maps of innervation (innervation domains, see Materials and Methods and Lübke et al. 2003). Average dendritic length density maps were created from a sample of 25 L2/3 pyramidal cells and 36 L4 spiny neurons, respectively. These prototypic density maps were duplicated for neighboring columns (cf., Materials and Methods). The axonal length density distributions of local, lateral, and translaminal L2/3-to-L4/5 inhibitors were multiplied with the 2 dendritic postsynaptic distributions, respectively. To ease comparison, innervation probability maps were normalized to the maximal value occurring in the set of innervation patterns. The resulting putative innervation maps for the 3 types of interneurons with corresponding axonal projections are shown in Figure 6B,C. The innervation maps for L1 inhibitors and chandelier neurons are depicted in Figure 7B,C.

Local inhibitors showed high putative innervation probabilities in L2/3 of the home column, only (Fig. 6B, top panel). The innervation domain of lateral inhibitors extended to the home and adjacent column in L2/3 (Fig. 6B, middle panel). Translaminal L2/3-to-L4/5 inhibitors showed only small local innervation probabilities. They had a peak in layer 4 for the innervation of L4 spiny neurons (Fig. 6C, bottom panel). L4

spiny stellate cells were, in turn, not significantly innervated by any of the other types of interneurons, (Fig. 6C, top and middle panels). The innervation probability of L1 inhibitors extended to the apical tufts of L2/3 pyramidal cells (shown in Fig. 7B, top panel). Neither of the other types of interneurons showed significant innervation probability in L1 (cf., Fig. 6B). Two Chandelier neurons had a high putative innervation probability for axon initial segments in L2/3 of the home column, only (Fig. 7B, bottom panel).

Discussion

The present study provides a quantitative reference frame for the contribution of inhibitory interneurons in the supra-granular layers to the signal flow in columns of the somatosensory barrel cortex. The main result is a quantitative definition of neuronal correlates of local, lateral, and translaminal inhibition with reference to the anatomical constraints of cortical columns.

Effects of Local and Lateral Inhibitors

The main criterion for the segregation into projection types was the maximum lateral and vertical extent of a significant part of a neuron's axonal arbor with reference to the borders of cortical columns. If an AP is elicited in a lateral inhibitor neuron, IPSPs can be monosynaptically evoked also in neurons located in neighboring columns. Local inhibitors, in contrast, do not affect neurons in other columns via monosynaptic connections. In this sense, the present definition of inhibitory projection types reflects the maximum "inhibitory territory" of a neuron.

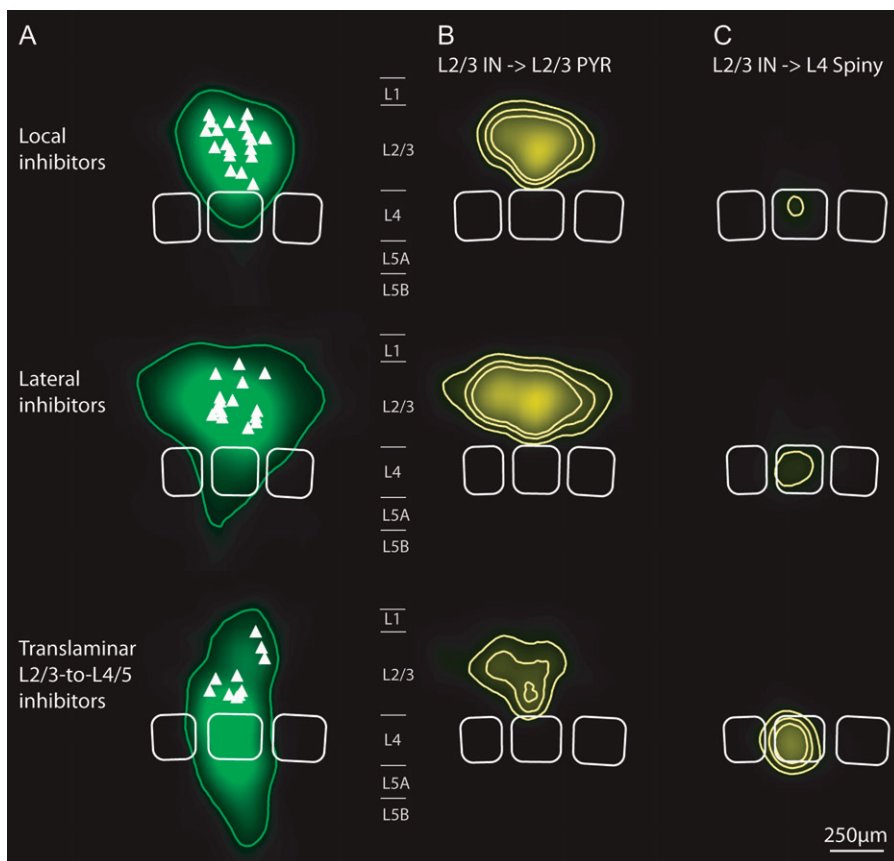


Figure 6. Average axonal projections for local, lateral, and translaminal L2/3-to-L4/5 inhibitors and corresponding innervation domains. (A) Maps of axonal path length density, averaged for local inhibitors ($n = 20$, top panel), lateral inhibitors ($n = 15$, middle panel), and translaminal L2/3-to-L4/5 inhibitors ($n = 10$, bottom panel) and aligned to the average barrel pattern for each type (white outlines). Isodensity contours that contained 90% of the total axonal length density were superimposed (green lines). Soma locations are indicated by white triangles. Maps were sampled at 50×50 voxel size, convolved with a Gaussian kernel and interpolated 10-fold (cf., Materials and methods). (B) Maps of average putative innervation domains for local, lateral, and translaminal L2/3-to-L4/5 inhibitors (top to bottom). At each point in the map, axonal density was multiplied with the average dendritic density of a sample of 25 L2/3 pyramidal neurons in the home and neighboring columns, each. Yellow lines are 3 isodensity contours normalized to the peak innervation density of all innervation maps for comparison. Note the extent of innervation domains of lateral inhibitors to the neighboring columns (middle panel). Both local and lateral inhibitors show innervation domains that exclude L1 (top and middle panels, compare Fig. 7). (C) Average putative innervation domains for the 3 types projecting to L4 spiny neurons. Average dendritic maps of 36 L4 spiny neurons were computed, and the innervation density was calculated as above. Note that only translaminal L2/3-to-L4/5 inhibitors show significant innervation probability in L4 (bottom panel). The innervation domain of lateral inhibitors (B, middle panel) suggests an asymmetry toward the “left” neighboring column. In the thalamocortical slice preparation, however, a clear identification of rows or arcs is not possible (cf., Land and Kandler 2002).

Table 1

Summary of axonal parameters, sorted by axonal types

Types		Verticality ratio	Laterality (a.u.)	Laterality ratio	Lateral extent of axon beyond home column (home column width)	Total axonal length (mm)
Local inhibitors	($n = 20$)	$0.06 \pm 89\%$	$0.15 \pm 58\%$	$0.07 \pm 98\%$	$0.42 \pm 53\%$	$18 \pm 54\%$
Lateral inhibitors	($n = 15$)	$0.1 \pm 91\%$	$0.56 \pm 36\%$	$0.28 \pm 44\%$	$1.5 \pm 40\%$	$24 \pm 46\%$
Translaminal L2/3-to-L4/5 inhibitors	($n = 10$)	$0.51 \pm 39\%$	$0.07 \pm 59\%$	$0.02 \pm 122\%$	$0.23 \pm 60\%$	$14 \pm 80\%$
L1 inhibitors	($n = 4$)	$0.01 \pm 147\%$	$0.38 \pm 51\%$	$0.21 \pm 64\%$	$0.92 \pm 50\%$	$23 \pm 36\%$
All types and ungrouped	($n = 51$)	$0.16 \pm 130\%$	$0.27 \pm 90\%$	$0.13 \pm 106\%$	$0.73 \pm 90\%$	$20 \pm 55\%$

Note that the measure of laterality (Fig. 1) is a linear combination of the laterality ratio and the lateral extent of the axon in units of the home column width. (The linear weights were 1 and 2, respectively, which approximated the first principal component of laterality ratio and lateral extent in our sample.) Values are mean \pm standard deviation (SD). SD is reported in percentage of mean to allow comparison of homogeneity between parameters and types.

Both L2/3 local inhibitors and L2/3 lateral inhibitors (via the part of their axon extended to L2/3 of the home column) could contribute to the low rates of AP firing in supragranular layer pyramidal neurons that was reported in vivo in response to sensory stimuli (Brecht et al. 2003; deKock et al. 2007; Kerr et al. 2007; Sarid et al. 2007). For such a dampening effect of L2/3 interneurons on L2/3 pyramidal neurons, the L2/3

interneurons would have to be activated near-synchronously by excitatory neurons in L4. In fact, efficient excitatory connections from L4 to L2/3 interneurons have been reported in an accompanying study (Helmstaedter, Staiger et al. 2008). Thus, when L4 excitatory neurons are activated in response to a sensory stimulus and in turn generate suprathreshold responses in L2/3 local inhibitors, the calculated innervation

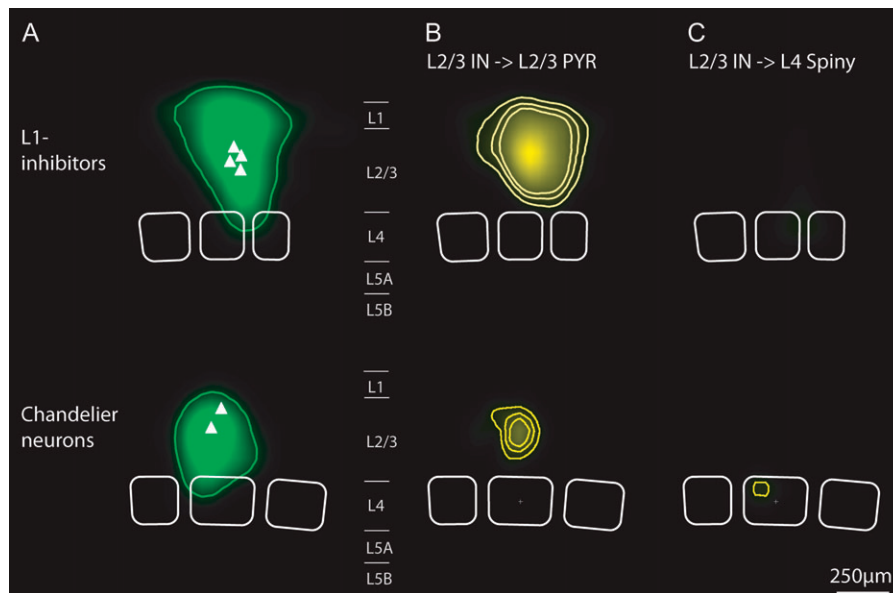


Figure 7. Average axonal projections of L1 inhibitors and chandelier neurons and corresponding innervation domains. (A) Maps of average axonal length density computed as in Figure 6. (B, C) Maps of putative innervation density of connections from L2/3 interneurons to excitatory neurons in layers 2/3 and 4. Note that L1 inhibitors have significant innervation probabilities at the apical tufts of L2/3 pyramidal neurons. L1 is, however, excluded by all other inhibitory projection types (cf., Fig. 6). For chandelier neurons, axonal initial segments of 20- μ m approximated length each were used as putative postsynaptic targets (Somogyi 1977) for innervation density calculation (cf., Materials and methods). Note that the axonal projection and putative innervation domain of the 2 chandelier neurons is confined to L2/3 of the home column.

domains of local inhibitors projecting to L2/3 pyramidal neurons (cf., Fig. 6) predict strong inhibitory effects on L2/3 pyramidal neurons in response to a sensory stimulus (for a more quantitative account of this argumentation, cf., Sarid et al. 2007; Helmstaedter, Staiger, et al. 2008).

The transcolumnar axonal projections of lateral inhibitors, which had a high innervation probability with L2/3 pyramidal neurons in neighboring columns (cf., Fig. 6B), could, in turn, constitute a correlate of the surround inhibition observed in barrel cortex (Kleinfeld and Delaney 1996; Derdikman et al. 2003). Suppression of principal whisker responses after neighboring column surround whisker stimulation requires neighboring column inhibition. Lateral inhibitors as reported in this study (cf., Fig. 6B) had in fact significant innervation probability of L2/3 pyramidal neurons in neighboring columns, allowing for a monosynaptic neighboring column surround inhibition.

The radius of surround inhibition as observed after principal whisker stimulation in a different study (Derdikman et al. 2003), however, was much larger (>700 μ m). This larger inhibitory surround could be mediated by polysynaptic transmission. The distribution of lateral inhibitors as shown in Figure 1C, however, may also suggest a type of “multicolumn lateral inhibitors” as interneurons with axonal projections that span more than 3 columns. Larger samples of interneurons may allow a quantitative definition of this type of interneuron.

Translaminar Inhibitors

The axonal projection of translaminar L2/3-to-L4/5 inhibitors, notably, is most dense in layer 4. The local (i.e., within L2/3) axonal projection of translaminar L2/3-to-L4/5 inhibitors comprises on average less than 50% of their total axonal projection. Thus, the projection of translaminar L2/3-to-L4/5 inhibitors can be interpreted as being more selective for layers within the home column. An extreme example is shown in Figure 1A. Analogous projections have not been observed for

lateral inhibitors in this sample. Lateral inhibition can consequently be interpreted as being selective for surround fields of different radius (Fox et al. 2003).

Axonal Field Span as a Surrogate Parameter

For the description of axonal projections with reference to putative cortical columns, axonal field span as a surrogate parameter has been routinely employed in the absence of anatomical landmarks of cortical columns (Valverde 1976; Fairén et al. 1984; Blatow et al. 2003; Karube et al. 2004; Krimer et al. 2005; Dumitriu et al. 2007). Given the geometry of cortical columns, for example, in the barrel field, where the horizontal diameter of a column (300–400 μ m) is comparable to the typical horizontal extent of axonal arbors of interneurons, axonal field span is not a strong predictor of intracolumnar versus transcolumnar axonal projection. Our data show that in fact, horizontal axonal field span alone cannot be used as a surrogate for axonal projections to neighboring columns (Fig. 3A). Rather, the data suggest that the position of the soma within the home column is relevant for the type of axonal projections: interneurons located at the borders of a column were more likely to show significant lateral axonal projections to neighboring columns (Fig. 3B). Thus, for the analysis of axonal projections with reference to cortical columns, the simultaneous identification of the column geometry was required and could not be substituted by measures of axonal field span, only.

L1 Inhibitors and Chandelier Neurons

We found by quantitative analysis of axon arbors that the axonal projection to L1 is a distinctive property for a small subset of L2/3 interneurons. None of the other interneuron types showed significant innervation probability in L1 (Fig. 7 vs. Fig. 6). L1 inhibitors were named by Ramón y Cajal, as “Martinotti cells” (Martinotti 1889; Ramón y Cajal 1904).

Martinotti cells were subject to post hoc analysis in a study by Wang et al. (2004) with, however, qualitative preselection of the neurons. For the definition of neuron classes, it is decisive to prove the distinctness in the unbiased population of interneurons. Recently, Martinotti cells have been demonstrated to provide direct inhibitory input to the stem and tuft of apical dendrites of L5 pyramidal cells (Silberberg and Markram 2007).

A specific property of the axonal projection (i.e., the presence of >100 vertically oriented axonal “cartridges”) was the defining criterion for 2 chandelier neurons in our sample as proposed previously (Somogyi 1977).

Relation to Previous Work

Few quantitative studies of axonal projection patterns of interneurons are available. In parallel to many qualitative descriptions (Ramón y Cajal 1904; Lorente de No 1938; Marin-Padilla 1969, 1970, 1972; Peters 1971; Valverde 1971; Szentagothai 1973; Marin-Padilla and Stibitz 1974; Jones 1975; Feldman and Peters 1978; Peters and Fairen 1978; Valverde 1978; Peters and Regidor 1981; DeFelipe and Fairen 1982; Gupta et al. 2000; Tamàs et al. 2003; Krimer et al. 2005), Sholl pioneered the quantitative evaluation of neuronal geometry (Sholl 1953, 1955). The quantitative analysis of target structures of axonal projections was initiated by Somogyi and coworkers (Somogyi and Cowey 1981; Somogyi et al. 1983). Recently, intrinsic axonal branching properties of interneurons were quantitatively analyzed in frontal cortex (Karube et al. 2004). The quantitative analysis was based on qualitative a priori classifications, which renders a comparison with our classifications speculative. In visual cortex, the relevance of axonal morphology for classification was recently shown in subpopulations of interneurons preselected by the expression of intracellular proteins (Dumitriu et al. 2007).

We used animals of age P20–P29 to avoid a critical developmental period in the second to third postnatal week (Huang et al. 1999; Mierau et al. 2004). Some studies used animals from approximately this period of time (P13–P16 or P14–P18) (e.g., Gibson et al. 1999; Gupta et al. 2000; Toledo-Rodriguez et al. 2005; Silberberg and Markram 2007).

Conclusions

Facing several possibilities of interneuron classifications, it seems decisive to begin with functionally most relevant parameters as classifiers. Here, we defined types of axonal projections as primary classifiers of interneurons. We use the term “type” for ensembles of neurons that share one functional property (here: their axonal projection pattern) but may vary with respect to other properties (such as their dendritic geometry, intrinsic electrical excitability, and expression of cytochemical markers). Subsequent more detailed classifications can make use of these less well-defined parameters. This approach is presented in this paper and subsequent studies (Helmstaedter et al. 2008a, 2008b; Helmstaedter, Staiger et al. 2008). It is expected that such quantitative approaches to interneuron identification will help to resolve structural correlates of cortical function with single-cell resolution in networks of tens of thousands of neurons.

Supplementary Material

Supplementary material can be found at <http://www.cercor.oxfordjournals.org/>.

Funding

This work was supported by the Max-Planck Society.

Notes

The authors would like to thank Drs Arnd Roth and Andreas Schaefer for many fruitful discussions, Drs Jochen Staiger and Andreas Schaefer for helpful comments on previous versions of the manuscript, and Ms Marlies Kaiser for expert technical assistance. *Conflict of Interest:* None declared.

Address correspondence to Moritz Helmstaedter, Department of Cell Physiology, Max-Planck Institute for Medical Research, Jahnstrasse 29, D-69120 Heidelberg, Germany. Email: moritz.helmstaedter@mpimf-heidelberg.mpg.de.

References

- Agmon A, Connors BW. 1991. Thalamocortical responses of mouse somatosensory (barrel) cortex in vitro. *Neuroscience*. 41:365–379.
- Beaulieu C, Kisvarday Z, Somogyi P, Cynader M, Cowey A. 1992. Quantitative distribution of GABA-immunopositive and -immunonegative neurons and synapses in the monkey striate cortex (area 17). *Cereb Cortex*. 2:295–309.
- Blatow M, Rozov A, Katona I, Hormuzdi SG, Meyer AH, Whittington MA, Caputi A, Monyer H. 2003. A novel network of multipolar bursting interneurons generates theta frequency oscillations in neocortex. *Neuron*. 38:805–817.
- Brecht M, Roth A, Sakmann B. 2003. Dynamic receptive fields of reconstructed pyramidal cells in layers 3 and 2 of rat somatosensory barrel cortex. *J Physiol*. 553:243–265.
- Cauli B, Porter JT, Tsuzuki K, Lambollez B, Rossier J, Quenet B, Audinat E. 2000. Classification of fusiform neocortical interneurons based on unsupervised clustering. *Proc Natl Acad Sci USA*. 97:6144–6149.
- de Kock CP, Bruno RM, Spors H, Sakmann B. 2007. Layer- and cell-type-specific suprathreshold stimulus representation in rat primary somatosensory cortex. *J Physiol*. 581:139–154.
- Derdikman D, Hildesheim R, Ahissar E, Arieli A, Grinvald A. 2003. Imaging spatiotemporal dynamics of surround inhibition in the barrels somatosensory cortex. *J Neurosci*. 23:3100–3105.
- DeFelipe J, Fairen A. 1982. A type of basket cell in superficial layers of the cat visual cortex. A Golgi-electron microscope study. *Brain Res*. 244:9–16.
- Doty HU, Zieglgänsberger W. 1990. Visualizing unstained neurons in living brain slices by infrared DIC-videomicroscopy. *Brain Res*. 537:333–336.
- Douglas RJ, Martin KAC. 2007. Mapping the matrix: the ways of neocortex. *Neuron*. 56:226–238.
- Dumitriu D, Cossart R, Huang J, Yuste R. 2007. Correlation between axonal morphologies and synaptic input kinetics of interneurons from mouse visual cortex. *Cereb Cortex*. 17:81–91.
- Fairen A, DeFelipe J, Regidor J. 1984. Nonpyramidal neurons. In: Peters A, Jones EG, editors. *Cerebral cortex: cellular components of the cerebral cortex*. New York: Plenum Press. p. 206–211.
- Feldman ML, Peters A. 1978. The forms of non-pyramidal neurons in the visual cortex of the rat. *J Comp Neurol*. 179:761–793.
- Feldmeyer D, Egger V, Lübke J, Sakmann B. 1999. Reliable synaptic connections between pairs of excitatory layer 4 neurones within a single ‘barrel’ of developing rat somatosensory cortex. *J Physiol*. 521:169–190.
- Feldmeyer D, Lübke J, Sakmann B. 2006. Efficacy and connectivity of intracolumnar pairs of layer 2/3 pyramidal cells in the barrel cortex of juvenile rats. *J Physiol*. 575:583–602.
- Fox K, Wright N, Wallace H, Glazewski S. 2003. The origin of cortical surround receptive fields studied in the barrel cortex. *J Neurosci*. 23:8380–8391.
- Gibson JR, Beierlein M, Connors BW. 1999. Two networks of electrically coupled inhibitory neurons in neocortex. *Nature*. 402:75–79.

- Gilbert CD, Wiesel TN. 1979. Morphology and intracortical projections of functionally characterised neurones in the cat visual cortex. *Nature*. 280:120-125.
- Goldreich D, Peterson BE, Merzenich MM. 1998. Optical imaging and electrophysiology of rat barrel cortex. II. Responses to paired-vibrissa deflections. *Cereb Cortex*. 8:184-192.
- Gonchar Y, Turney S, Price JL, Burkhalter A. 2002. Axo-axonic synapses formed by somatostatin-expressing GABAergic neurons in rat and monkey visual cortex. *J Comp Neurol*. 443:1-14.
- Gupta A, Wang Y, Markram H. 2000. Organizing principles for a diversity of GABAergic interneurons and synapses in the neocortex. *Science*. 287:273-278.
- Hausser M, Spruston N, Stuart GJ. 2000. Diversity and dynamics of dendritic signaling. *Science*. 290:739-744.
- Helmstaedter M, de Kock CPJ, Feldmeyer D, Bruno RM, Sakmann B. 2007. Reconstruction of an average cortical column in silico. *Brain Res Rev*. 55:193-203.
- Helmstaedter M, Sakmann B, Feldmeyer D. 2008b. L2/3 interneuron groups defined by multi-parameter analysis of axonal projection, dendritic geometry and electrical excitability. *Cereb Cortex*. doi:10.1093/cercor/bhn130.
- Helmstaedter M, Sakmann B, Feldmeyer D. 2008a. The relation between dendritic geometry, electrical excitability, and axonal projections of L2/3 interneurons in rat barrel cortex. *Cereb Cortex*. doi:10.1093/cercor/bhn138.
- Helmstaedter M, Staiger JF, Sakmann B, Feldmeyer D. 2008. Differential recruitment of layer 2/3 interneuron groups by layer 4 input in single columns of rat somatosensory cortex. *J Neurosci*. 28:8273-8284.
- Hensch TK, Fagiolini M, Mataga N, Stryker MP, Baekkeskov S, Kash SF. 1998. Local GABA circuit control of experience-dependent plasticity in developing visual cortex. *Science*. 282:1504-1508.
- Houser CR, Hendry SH, Jones EG, Vaughn JE. 1983. Morphological diversity of immunocytochemically identified GABA neurons in the monkey sensory-motor cortex. *J Neurocytol*. 12:617-638.
- Howard A, Tamas G, Soltesz I. 2005. Lighting the chandelier: new vistas for axo-axonic cells. *Trends Neurosci*. 28:310-316.
- Huang ZJ, Kirkwood A, Pizzorusso T, Porciatti V, Morales B, Bear MF, Maffei L, Tonegawa S. 1999. BDNF regulates the maturation of inhibition and the critical period of plasticity in mouse visual cortex. *Cell*. 98:739-755.
- Jones EG. 1975. Varieties and distribution of non-pyramidal cells in the somatic sensory cortex of the squirrel monkey. *J Comp Neurol*. 160:205-267.
- Karube F, Kubota Y, Kawaguchi Y. 2004. Axon branching and synaptic bouton phenotypes in GABAergic nonpyramidal cell subtypes. *J Neurosci*. 24:2853-2865.
- Kerr JN, de Kock CP, Greenberg DS, Bruno RM, Sakmann B, Helmchen F. 2007. Spatial organization of neuronal population responses in layer 2/3 of rat barrel cortex. *J Neurosci*. 27:13316-13328.
- Kleinfeld D, Delaney KR. 1996. Distributed representation of vibrissa movement in the upper layers of somatosensory cortex revealed with voltage-sensitive dyes. *J Comp Neurol*. 375:89-108.
- Krimer LS, Zaitsev AV, Czanner G, Kroner S, Gonzalez-Burgos G, Povysheva NV, Iyengar S, Barrionuevo G, Lewis DA. 2005. Cluster analysis-based physiological classification and morphological properties of inhibitory neurons in layers 2-3 of monkey dorsolateral prefrontal cortex. *J Neurophysiol*. 94:3009-3022.
- Kyriazi HT, Carvell GE, Brumberg JC, Simons DJ. 1996. Quantitative effects of GABA and bicuculline methiodide on receptive field properties of neurons in real and simulated whisker barrels. *J Neurophysiol*. 75:547-560.
- Land PW, Kandler K. 2002. Somatotopic organization of rat thalamocortical slices. *J Neurosci Methods*. 119:15-21.
- Larkum ME, Zhu JJ, Sakmann B. 1999. A new cellular mechanism for coupling inputs arriving at different cortical layers. *Nature*. 398:338-341.
- Lorente de No R. 1938. Cerebral cortex: architecture, intracortical connections, motor projections (chapter 15). In: Fulton JF, editor. *Physiology of the nervous system*. Oxford: Oxford University Press. p. 288-313.
- Lübke J, Egger V, Sakmann B, Feldmeyer D. 2000. Columnar organization of dendrites and axons of single and synaptically coupled excitatory spiny neurons in layer 4 of the rat barrel cortex. *J Neurosci*. 20:5300-5311.
- Lübke J, Roth A, Feldmeyer D, Sakmann B. 2003. Morphometric analysis of the columnar innervation domain of neurons connecting layer 4 and layer 2/3 of juvenile rat barrel cortex. *Cereb Cortex*. 13:1051-1063.
- Lund JS. 1973. Organization of neurons in the visual cortex, area 17, of the monkey (*Macaca mulatta*). *J Comp Neurol*. 147:455-496.
- Marin-Padilla M. 1969. Origin of the pericellular baskets of the pyramidal cells of the human motor cortex: a Golgi study. *Brain Res*. 14:633-646.
- Marin-Padilla M. 1970. Prenatal and early postnatal ontogenesis of the human motor cortex: a golgi study. II. The basket-pyramidal system. *Brain Res*. 23:185-191.
- Marin-Padilla M. 1972. Double origin of the pericellular baskets of the pyramidal cells of the human motor cortex: a Golgi study. *Brain Res*. 38:1-12.
- Marin-Padilla M, Stibitz GR. 1974. Three-dimensional reconstruction of the basket cell of the human motor cortex. *Brain Res*. 70:511-514.
- Martinotti C. 1889. Contributo allo studio della corteccia cerebrale, ed all'origine central dei nervi. *Ann Freniatri Sci Affini*. 1:14-381.
- Mierau SB, Meredith RM, Upton AL, Paulsen O. 2004. Dissociation of experience-dependent and -independent changes in excitatory synaptic transmission during development of barrel cortex. *Proc Natl Acad Sci USA*. 101:15518-15523.
- Mountcastle VB. 1957. Modality and topographic properties of single neurons of cat's somatic sensory cortex. *J Neurophysiol*. 20:408-434.
- Mountcastle VB. 1997. The columnar organization of the neocortex. *Brain*. 120:701-722.
- Mountcastle VB. 2003. Introduction. *Computation in cortical columns*. *Cereb Cortex*. 13:2-4.
- Peters A. 1971. Stellate cells of the rat parietal cortex. *J Comp Neurol*. 141:345-373.
- Peters A, Fairen A. 1978. Smooth and sparsely-spined stellate cells in the visual cortex of the rat: a study using a combined Golgi-electron microscopic technique. *J Comp Neurol*. 181:129-171.
- Peters A, Regidor J. 1981. A reassessment of the forms of nonpyramidal neurons in area 17 of cat visual cortex. *J Comp Neurol*. 203:685-716.
- Pinto DJ, Brumberg JC, Simons DJ. 2000. Circuit dynamics and coding strategies in rodent somatosensory cortex. *J Neurophysiol*. 83:1158-1166.
- Pinto DJ, Hartings JA, Brumberg JC, Simons DJ. 2003. Cortical damping: analysis of thalamocortical response transformations in rodent barrel cortex. *Cereb Cortex*. 13:33-44.
- Pouille F, Scanziani M. 2001. Enforcement of temporal fidelity in pyramidal cells by somatic feed-forward inhibition. *Science*. 293:1159-1163.
- Ramón y Cajal S. 1904. *Textura del sistema nervioso del hombre y de los vertebrados*. Madrid (Spain): Imprenta N. Moya.
- Rose D, Blakemore C. 1974. Effects of bicuculline on functions of inhibition in visual cortex. *Nature*. 249:375-377.
- Sarid L, Bruno R, Sakmann B, Segev I, Feldmeyer D. 2007. Modeling a layer 4-to-layer 2/3 module of a single column in rat neocortex: interweaving in vitro and in vivo experimental observations. *Proc Natl Acad Sci USA*. 104:16353-16358.
- Sholl DA. 1953. Dendritic organization in the neurons of the visual and motor cortices of the cat. *J Anat*. 87:387-406.
- Sholl DA. 1955. The organization of the visual cortex in the cat. *J Anat*. 89:33-46.
- Silberberg G, Markram H. 2007. Disynaptic inhibition between neocortical pyramidal cells mediated by Martinotti cells. *Neuron*. 53:735-746.

- Sillito AM. 1975. The contribution of inhibitory mechanisms to the receptive field properties of neurones in the striate cortex of the cat. *J Physiol.* 250:305-329.
- Soltesz I. 2006. Diversity in the neuronal machine: order and variability in interneuronal microcircuits. Oxford, New York: Oxford University Press.
- Somogyi P. 1977. A specific 'axo-axonal' interneuron in the visual cortex of the rat. *Brain Res.* 136:345-350.
- Somogyi P, Cowey A. 1981. Combined Golgi and electron microscopic study on the synapses formed by double bouquet cells in the visual cortex of the cat and monkey. *J Comp Neurol.* 195:547-566.
- Somogyi P, Freund TF, Cowey A. 1982. The axo-axonic interneuron in the cerebral cortex of the rat, cat and monkey. *Neuroscience.* 7:2577-2607.
- Somogyi P, Kisvarday ZF, Martin KA, Whitteridge D. 1983. Synaptic connections of morphologically identified and physiologically characterized large basket cells in the striate cortex of cat. *Neuroscience.* 10:261-294.
- Stuart GJ, Dodt HU, Sakmann B. 1993. Patch-clamp recordings from the soma and dendrites of neurons in brain slices using infrared video microscopy. *Pflugers Arch.* 423:511-518.
- Szentagothai J. 1973. Synaptology of the visual cortex. In: Jung R, editor. *Handbook of sensory physiology.* New York: Springer-Verlag. p. 269-324.
- Szentagothai J, Arbib MA. 1974. Conceptual models of neural organization. *Neurosci Res Program Bull.* 12:305-510.
- Tamás G, Lőrincz A, Simon A, Szabadics J. 2003. Identified sources and targets of slow inhibition in the neocortex. *Science.* 299:1902-1905.
- Thorndike RL. 1953. Who belongs in the family? *Psychometrika.* 18:267-276.
- Toledo-Rodriguez M, Goodman P, Illic M, Wu C, Markram H. 2005. Neuropeptide and calcium-binding protein gene expression profiles predict neuronal anatomical type in the juvenile rat. *J Physiol.* 567:401-413.
- Valverde F. 1971. Short axon neuronal subsystems in the visual cortex of the monkey. *Int J Neurosci.* 1:181-197.
- Valverde F. 1976. Aspects of cortical organization related to the geometry of neurons with intra-cortical axons. *J Neurocytol.* 5:509-529.
- Valverde F. 1978. The organization of area 18 in the monkey. A Golgi study. *Anat Embryol (Berl).* 154:305-334.
- Van Essen D, Kelly J. 1973. Correlation of cell shape and function in the visual cortex of the cat. *Nature.* 241:403-405.
- Wang Y, Toledo-Rodriguez M, Gupta A, Wu C, Silberberg G, Luo J, Markram H. 2004. Anatomical, physiological and molecular properties of Martinotti cells in the somatosensory cortex of the juvenile rat. *J Physiol.* 561:65-90.
- Ward JH. 1963. Hierarchical grouping to optimize an objective function. *J Am Stat Assoc.* 58:236-244.
- Woolsey TA, Van der Loos H. 1970. The structural organization of layer IV in the somatosensory region (SI) of mouse cerebral cortex. The description of a cortical field composed of discrete cytoarchitectonic units. *Brain Res.* 17:205-242.